STRUCTURAL STRESS ANALYSIS AND RELIABILITY EVALUATION FOR A NEW SPEED REDUCER

Y.-T. Tsai*

Department of Mechanical Engineering
DeLin Institute of Technology
New Taipei, Taiwan

K.-H. Lin

Department of Mechanical Engineering
Tungnan University
New Taipei, Taiwan

ABSTRACT

Reducers are extensively used in many machines for reducing the speeds of mechanism. This paper proposed a new design of speed reducers to meet the performance requirements in high rigidness and large speed-reduction ratios. The movements of the reducer are designed based on the principles of differential displacements of the deceleration gear rings. The geometric models of the related components were designed using **CAD** software. The motions of mechanism were simulated for identifying the feasibility of designing including acquiring the kinematic properties. The mathematical models of structural stresses analysis were proposed so that the bending and contact stresses of the gear rings could be evaluated, accordingly. Finite element methods (**FEM**) were also used to analyze the structural stresses of the reducer. The studied results showed that the bending fracture of the gear rings would prior to its contacting fracture. The allowable loading of the reducer was then established according to the analyzed results of the maximum stresses on various transmitted torques. The methods of reliability evaluation were reported for considering the strength variation and calculating the reliabilities of the reducer at various loadings. The studied results are useful in structural design, stress analysis and reliability evaluation for developing high speed-reduction mechanisms.

Keywords: Design, Reducer, Reliability evaluation.

1. INTRODUCTION

Robots play a critical role on automatic production and are more and more common in industrial applications. The performance requirements of robots usually include positioning accuracy, geometric agility and a wide ranges of speed and torque outputs [1]. The speed reducers used in industrial robots were requested to own the properties, high speed-reduction ratios, large torque outputs and compact structure due to the functional requirements and the volume constraints. The properties of speed-reduction ratios play a key role in robot's performance outputs. An often used reducer in robots is the harmonic gear decelerators because it has the properties, small backlash, high transmission accuracy, large reduction ratio [2]. The existed problems of the harmonic gear decelerators are the rigidity inadequate as well as transmitted torques limited due to the flexible design of the gear rings [3]. The other applied one is the trochoidal gear reducers because of the advantages of high torsional rigidity, great load capacity and high shock-resistant ability. Shuting Li [4] explored the designing and strength of a trochoidal gear reducer. Although many types of reducers have been designed and used now, there are still many structural problems, such as motion analysis, stress and reliability evaluation, etc., have not been solved so far.

A new design based on differential displacements of the decelerated gear rings, named as Differential Reducer (**DR**), is proposed to satisfy the functional requirements such as high rigidness, large reduction ratios and compact structure. The **DR** is designed primarily consisting of three gear rings and one off-centre cam. It possesses better structural strength compared with the harmonic decelerators due to the rigid design of the gear rings. The function of high speed-reduction ratios is accom-

* Corresponding author (yttsai@dlit.edu.tw)

DOI : 10.1017/jmech.2016.96
Copyright © 2016 The Society of Theoretical and Applied Mechanics
https://doi.org/10.1017/jmech.2016.96 Published online by Cambridge University Press

plished by the differential displacements of the gear rings. Designing of the gear rings are the critical jobs in deciding the strength, precision and kinematic properties of the **DR**. The teeth of the gear rings are designed with profile shifted involute to treat the problems of engaging interference.

The power transmission of the **DR** is from the off-centre cam to the gear rings. The induced stresses of the gear rings primarily include both tooth root bending stresses and tooth surface contact stresses. The two stresses of the gear rings can be evaluated according to the theories of inner gear transmission. The classic methods of estimating bending stresses of gear teeth are by the Lewis equation, and contact stresses are by the Hertz equation [5]. There are many theories had been reported about gear designing, for example, Koisha *et al*. [6] presented the influence of friction on contact stress for small power transmission planetary gear box. The formulas of calculating bending and contact stresses of gears had been published in ISO 6336 [7, 8, 9]. Japanese Gear Manufacturer Association (JGMA) also reported the related formulas about gear designing [10]. The formulas always involve many unknown parameters which usually are determined by complex analyzed procedures. The values sometimes are uneasily given accurately due to professional information inadequate. A feasible method to simplify the complexities of analyzing on gear stress is by Computer Aided Design/Engineering **(CAD/CAE)** methods.

CAD/CAE is applied more and more common in supporting product design for prototype creation, motion analysis and stress evaluation. **ANSYS** is a method of Finite Element Analysis (**FEA**) which is extensively used in many fields for engineering stress analysis [11]. The DesignModeler in ANSYS offers a parametric design to generate the plain or solid geometric models. The geometric models are imported into the analyzed systems for meshing and implementing **FEA** [12]. **FEA** is sometimes slightly infeasible to obtain a solution due to sometimes slightly violating the constraints. The response surface methods can be used to replace the time-consuming finite element simulations to improve the efficiency of optimization. In addition, reliability is being emphasized more and more due to the increased complexity of modern engineering designs. Reliability design is fulfilled based on Stress-Strength Interference (**SSI**) theory and usually is performed in accompanying with optimization methods [13]. Several instances in combining engineering stress analysis and probabilistic design approach to perform reliability design had been reported in recent. For example, Tsai *et al*. [14] made use of the limited experimental data and the simulated stresses obtained by **FEA** to evaluate the fatigue life of dental implants. Integrating **CAD/CAE** with probabilistic theories to perform reliability optimization design for the arms of robots is another example [15].

In this paper, **CAD/CAE** is used as a tool to develop a new design of reducers which own high ratios of speed reduction. The parametric approach of designing is constructed by SolidWorks for the reducer so that the related components of the **DR** can be rapidly created according to the set values of the parameters. The motions of the **DR** are simulated for identifying the feasibility of designing and obtaining the kinematic properties. The mathematical models of structural stress are introduced to calculate the bending and contact stresses of the gear rings. The geometric models of the **DR** created in **CAD** software are loaded into **ANSYS** to perform structural stress analysis. Probabilistic design approach is presented to evaluate the reliabilities of the **DR** under different loadings so that the allowed loadings of the **DR** can be determined accordingly. The studied results offer useful information on designing, analyzing and evaluating for a new reducer possessing high speed-reduction ratios.

2. DIFFERENTIAL REDUCER (DR)

A new model of speed reducers is proposed to meet the properties of high rigidness, large reduction ratios and structure compactness. The geometric models of the reducers are constructed by **CAD** software so that the kinematic properties and structural stresses can be further investigated.

2.1 Design Scheme

The **DR** is designed based on the differential displacements of the gear rings. The working principles of the gear rings are similar to the movements of the sliding meter to the fixed meter of the traditional caliper. There are four components name as fixed gear ring, sliding gear ring, intermediary gear ring and one off-centre cam are enclosed in the reducer. The explosion drawings of the geometric structure of the **DR** are illustrated in Fig. 1. The intermediary ring is driven by the off-centre cam acted as power input to transmit the power to the sliding ring along with the fixed ring. The fixed and sliding rings are designed with different tooth numbers so that the slight displacements can be generated when the intermediary ring is rotating circling the center of the fixed ring. The differential movements are created when the teeth of the sliding ring are forced to align to the fixed ring due to the mating transmissions. The fixed ring is usually fixed on the support box for leading the intermediary ring rotating along with the form of planetary

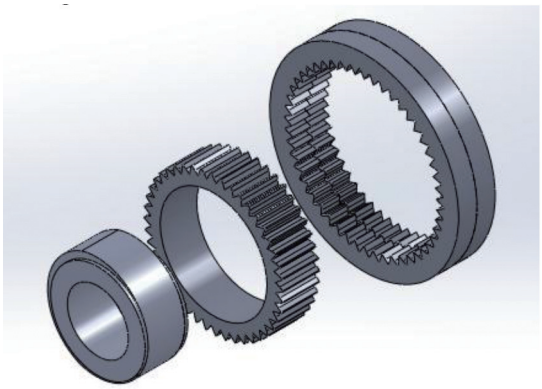


Fig. 1 Geometric structure of the differential reducer.

https://doi.org/10.1017/jmech.2016.96 Published online by Cambridge University Press

The ratios of speed-reduction are decided depending on the difference of the tooth numbers of the fixed and sliding gear rings.

The off-centre cam is installed in the intermediary ring inside which is driven by the power shaft. It drives the intermediary ring to generate planetary motions circling the fixed ring. The off-centre cam can be designed with counterweight at the other side to dispel the imbalance during running. The tooth shapes of the gear rings are designed with profile shifted involute for insuring the mating transmission no interference occurrence. The bearings of the power shaft can be settled at two sides of the gear box for compacting the structure. The tooth numbers of the fixed and sliding rings are decided according to the ratios of speed reduction. The ratios of speed reduction can be expressed as

$$s = \frac{z_s - z_c}{z_s} \tag{1}$$

where z_s, z_c stand for the tooth numbers of the sliding and the fixed gears, respectively.

The geometric models of the **DR** are designed using SolidWorks software. The gear rings are created by parametric design based on involute profile of full depth. Parametric design means that the physical shapes are driven by the feature values assigned to the attributes (primarily dimensions) of gear teeth. Figure 2 illustrates the creation of involute profile of the gear teeth.

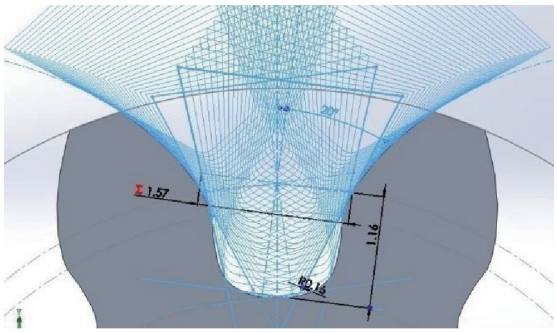


Fig. 2 Creation of involute gear profile.

The sizes of tooth shape of the gear rings are decided depending on transmitted torques and the volume constraints. For the purpose of structure compactness, the sliding ring and the sustained bearings can be designed as a whole for shortening the length of the reducer.

2.2 Motion Simulation

Motion simulation is to identify the accuracy of designing as well as to avoid interference occurrence. In this example, the gear rings including fixed, sliding and intermediary rings are designed with module m = 1, pressure angle θ = 20°. The tooth numbers of fixed, sliding and intermediary gear rings are set to {100, 101, 80}, respectively. The ratios of speed-reduction at the designed variables would be s = 1/101 according to Eq. (1). The off-centre cam was designed according to the geometric needs of motion. The off-centre distance is defined as

$$e = \frac{D_s - D_c}{2} \tag{2}$$

where D_s, D_c are the pitch diameters the sliding and the fixed gears, respectively. The plain perspective of the **DR** is shown in Fig. 3.

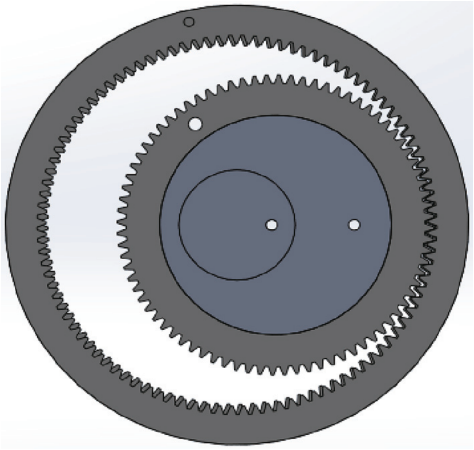


Fig. 3 Plain perspective of the **DR**.

The motion simulation is carried out using SolidWorks Motion module including interference check and kinematic properties analyzing. It is done by setting the combined conditions of the related components in Motion module. The simulated results showed that the mechanism has a large speed reduction and no interference occurrence on the gear rings. In this example, the rotational speeds of the off-centre cam are set to n_i = 60 rpm (360°/s) and the simulated time is set to 4 sec. The simulated results of kinematic velocities for the components are shown in Fig. 4. The intermediary ring is -15 rpm (-90°/s) and the sliding ring is 0.594 rpm (-3.56°/s) which is equal to the value of equation calculation in speed reduction.

To observe the varying of power transmission of the mechanism, a loading is added on the sliding ring to simulate the mechanical benefits. The power torques are set on the off-centre cam as well as the loadings on the sliding ring. The simulated results for the power torques and the power consuming under the loadings 0 – 200 Nm are shown in Fig. 5. The power torque at loading 200 Nm is 1.98 Nm and the power consuming is 12 watt. The value of mechanical benefits is 101 which is equal to the speed reduction ratio.

The simulated results showed that the needed power torques and the loadings exhibited a linear relationship as well as the power consuming to the loadings. The simulated results identify the accuracy of mechanism motion also provide the information of power needs of the driven motor for various loading conditions.

3. STRUCTURAL STRESSES ANALYSIS

Power transmission of the **DR** is starting from the

https://doi.org/10.1017/jmech.2016.96 Published online by Cambridge University Press

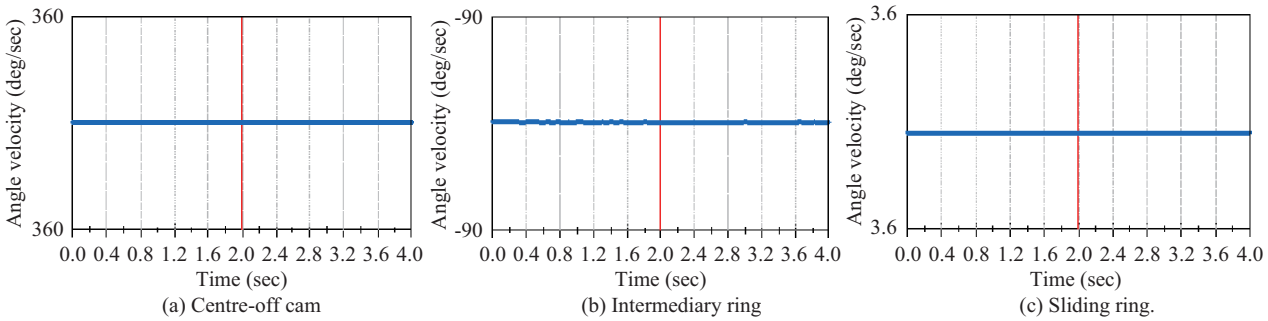


Fig. 4 Angle velocities of the components.

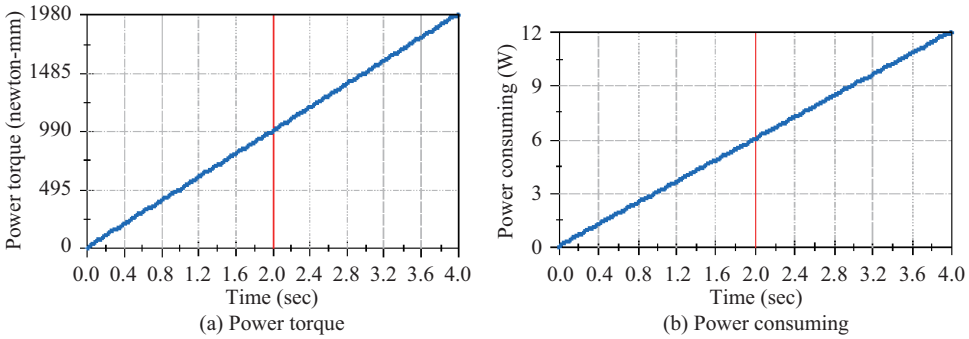


Fig. 5 Power varying of loadings from 0 to 200 Nm.

power shaft -> the off-centre cam -> the intermediary ring -> the sliding ring (the output). The structural weaknesses of the **DR** may occur at the teeth of the gear rings. The failure modes of the gear rings are either gear teeth breakage when the transmitted torques over the material strengths, or gear tooth worn out after a period of time using. The former is caused due to the tooth root bending stresses over the material strengths; the latter is caused by repeated contact stresses.

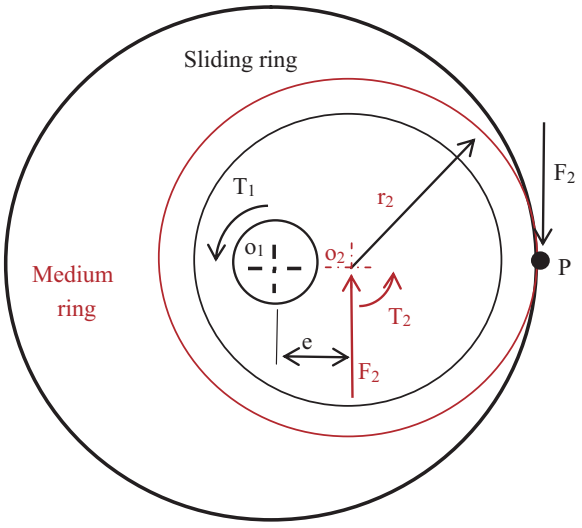


Fig. 6 Loading analysis of the mechanism

The acted forces of the mechanism can be decided according to force equivalent as illustrated in Fig. 6. The point P is the contact point of pitch circle of the intermediary and sliding rings. The input torques (T_1) are acting on the rotational center of the off-centre cam (O_1). The torques are transmitted to the intermediary ring by cylindrical contact to drive the sliding ring which is the power outputs. A reacted force (F_2) should be arisen at the contact point of the engaging position due to the loadings. The input torques (T_1) can then be transformed into 2 components (T_2, F_2) as shown in Fig. 6 which are acting on the center of the intermediary ring. The perpendicular force can be evaluated according to force equivalence as

$$F_2 = \frac{T_1}{(r_2 + e)} \tag{3}$$

The moment acting on the intermediary ring can also be obtained according to moment equivalence as

$$T_2 = \frac{r_2}{(r_2 + e)} T_1 \tag{4}$$

The input torques are converted into two components acting on the gear rings so that the problems can be transformed into paired transmission of inner gears. Focusing on gear transmission, the ISO standards, 6336, had reported the methods in calculating tooth surface contact stress and tooth root bending stress for a pair of spur gears and helical gears. The formula of contact stress calculation for a pair of spur gears and helical gears having contact ratios in the range $1 < c < 2$ is defined as

$$\sigma_c = Z_P Z_O Z_E Z_C Z_H \sqrt{\frac{F_t}{bd} \cdot \frac{(\mu \pm 1)}{u} K_A K_D K_\alpha K_\beta} \tag{5}$$

https://doi.org/10.1017/jmech.2016.96 Published online by Cambridge University Press

where the "+" symbol in equations applies to two external gears in mesh, and the "–" symbol is used for an internal gear and an external gear mesh. The other symbols are

Z_P: The single pair tooth contact factor of the wheel.
Z_O: The zone factor, the flank curvatures at the pitch point and transforms tangential load at the reference cylinder to tangential load at the pitch cylinder.
Z_E: The elasticity factor, the specific properties of the material.
Z_C: The contact ratio factor, the influence of the effective length of the lines of contact.
Z_H: The helix angle factor.
K_A: The application factor, the load increment due to externally influenced variations of input or output torque.
K_D: The dynamic factor, the load increments due to internal dynamic effects.
K_α: The transverse load factor for contact stress, the uneven load distribution in the transverse direction resulting, for example, from pitch deviation.
K_β: The face load factor for contact stress, the uneven distribution of load over the face width, due to mesh misalignment caused by inaccuracies in manufacture, elastic deformations, etc.
F_t: The nominal tangential load (N)
d: The reference diameter (mm)
b: The face width (mm)
u: The gear ratio (Z_2/Z_1)

On the other hand, the methods of calculating tooth root bending stress for a pair of spur gears and helical gears is also defined as

$$\sigma_F = \frac{F_t}{bm_n} Y_F Y_s Y_{DT} Y_H Y_B K_A K_D K_\alpha K_\beta \tag{6}$$

The detailed meanings of the symbols just as the contact stress formula can refer to ISO 6336-3 [9]. The two formulas involve a lot of unknown parameters which always are decided involving many complex analyzed processes. The detailed methods for giving the parametric values can refer to the data reported in Ref. [7][9][10].

An example of calculating contact stresses of the gear rings is reported to depict the applications of the mathematical models. Considering the input torque $T_1 = 200$ Nm, the moment acted on the gear ring would be $T_2 = 160$ Nm according to loading analysis. Here, the parameters (F_t, Z, d, b, u, Z_P, Z_O, Z_E, Z_C, Z_H, K_A, K_V, K_α, K_β) are set to (4000, 80, 80, 12, 1.25, 1, 2.5, 186.96, 0.97, 1, 1, 1, 1, 1), respectively. The parametric values are the same as the ones used in Ref. [5] in calculating the bending and contact stress of spur gears. Substituting these values into Eq. (5), the evaluated value of contact stress for the gear rings would be σ_c = **413.9 MPa**. Similarly, the bending stresses can also be obtained by substituting the values into Eq. (6). However, the stress evaluations singly by the above equation are inadequate to describe the stresses of the gear rings of the **DR** because the perpendicular loadings don't be considered in the equations.

4. STRUCTURAL STRESS OF THE DR

Structural stresses of the gear rings are analyzed using finite element methods for simultaneously considering the effects of the perpendicular forces and the moments. The **ANSYS** is a powerful tool of **FEA** which is used for analyzing structural stresses of the gear stresses. The analyzed results provide the strength information of the **DR** so that the design variables can be determined accordingly.

The geometric models of the **DR** were loaded into **ANSYS** to perform structural stress analysis. The 3D geometric models are processed by DesignModeler to convert the 3D models into surface models. The off-centre cam is suppressed for simplifying the problem. The input torque acting on the off-centre cam is substituted with the bearing force and the moment acting on the gear rings. Plane stress analysis is done for the gear rings. Plane stress analysis chosen is due to the facts: (i) the geometry of the gear rings along the axis of rotation are uniform and there is absence of axial loading; (ii) the assembly error is not modeled in this study; (iii) the stresses generated on the axial direction can be ignored.

The induced bending and contacting stresses of the gear rings are the major concerned problems. The material of the gear rings are set to structural steel (S35C) whose material properties are listed in Table 1. The augmented lagrange formulation method is selected for analyzing because it is the best suitable one among the available methods for frictional contact types which belong to nonlinear analysis. The connections of the contact positions of the teeth are set to frictional contact where the frictional coefficient is set to 0.2. The connected behavior is set to symmetric including the pinball radius to 0.2 mm.

Table 1 Material properties

Property	Value	Unit
Density	7850	Kg m^-3
Isotropic Secant Coefficient of Thermal Expansion		
Isotropic Elasticity		
Derive from	Young'…	
Young's Modulus	2E+05	MPa
Possion's Ratio	0.3	
Bulk Modulus	1.6667E+11	Pa
Shear Modulus	7.6923E+10	Pa
Alternating Stress Mean Stress	Tabular	
Strain-Life Parameters		
Tensile Yield Strength	304	MPa
Compressive Yield Strength	304	MPa
Tensile ltimate Strength	510	MPa

The meshes of the mating areas of the teeth are strengthened by setting the element size to 0.1 mm for

https://doi.org/10.1017/jmech.2016.96 Published online by Cambridge University Press

Table 2 Details of meshing

⊟	**Defaults**	
	Physics Preference	Mechanical
	☐ Relevance	100
⊟	**Sizing**	
	Use Advanced Size Function	On: Curvature
	Relevance Center	Fine
	Initial Size Seed	Active Assembly
	Smoothing	Medium
	Span Angle Center	Coarse
	☐ Curvature Normal Angle	Default (30.0°)
	☐ Min Size	Default (0.6282…
	☐ Max Face Size	Default (3.1414…
	☐ Growth Rate	Default
	Minimum Edge Length	0.647170 mm
⊞	**Inflation**	
⊞	**Patch Conforming Options**	
⊞	**Advanced**	
⊞	**Defeaturing**	
⊞	**Staistics**	

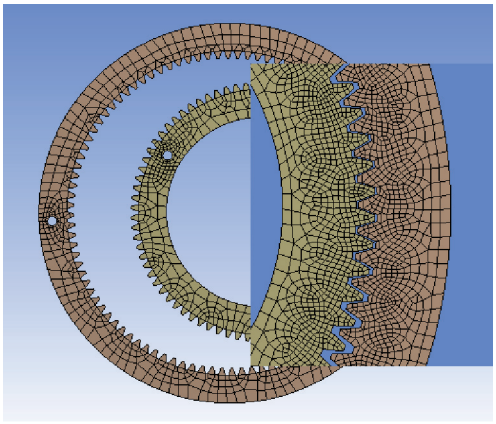


Fig. 7 Meshing of the gear rings.

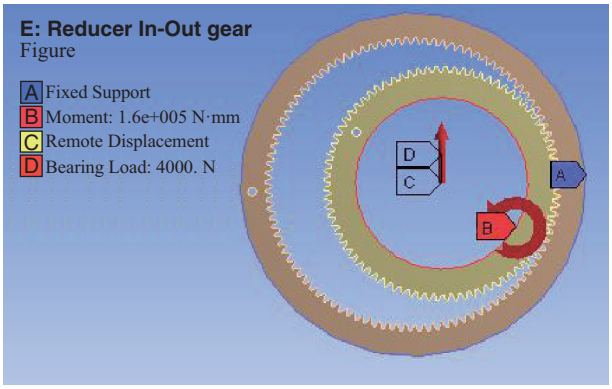


Fig. 8 The setting of supports and loadings.

obtaining the better solutions. The relevance and the methods of meshing are largely affecting the analyzed results. Here, the mesh control is set to quadrilateral dominant and the relevance is set to 100 for obtaining the fine analyzed results. The details of meshing are shown in Table 2. According to these set values, the meshing of the parts is shown in Fig. 7.

The outer ring is set to fixed support to simulate the external loading and the inner ring is set to remote displacement. The acted forces of the gear rings are decided according to loading analysis reported in previous section. The bearing force and the moment acting on the inner ring are set to 4000 N and 160 Nm, respectively, for the input torque being 200 Nm. The setting of the loadings and the supports of this example are shown in Fig. 8. The analyzed results for equivalent stresses i.e. contact stresses, are shown in Fig. 9. The maximum stress is about **429 MPa** occurring at the engaged positions of the teeth. The value is a little bigger than the value obtained by formula computation in previous section. This is reasonable since the loadings enclose the bearing force. The contact stresses are the sources of gear teeth worn out.

On the other hand, the bending stresses of tooth root are expressed with maximum principle stress. The analyzed results of maximum principle stress for this example are about **254 MPa** as shown in Fig. 10. The bending stresses are the causes resulting in gear tooth breakage.

The total deformations of the gear rings under the loadings can also be rated as shown in Fig. 11. The maximum deformations occurring at the inner ring is about **0.06 mm**. The force convergence of this example is shown in Fig. 12.

Normally, the analyzed results in **FEA** are largely related to the mesh setting. To identify the accuracy of analyzing, the convergence conditions of stresses at various numbers of nods are studied based on the meshes of quadrilateral dominant. The maximum equivalent and principle stresses at various element sizes are recorded in Table 3. The converged conditions about the maximum equivalent and principle stresses are illustrated in Fig. 13. The results show that the maximum equivalent and principle stresses would converge to one value, respectively, following the increasing of node numbers. This condition represents that the analyzed results are acceptable. The results imply that making use of **FEA** to evaluate the structural stresses of **DR** is feasible.

5. RELIABILITY DESIGN

Reliability is the probability that a system or component is performing its required function at a given time point or over a stated period of time when it operates under a set of prescribed conditions [16]. A study about reliability analysis of dental implants was proposed in Ref. [17]. Here, reliability is used to express the safeties of the **DR** under various loading torques.

5.1 Reliability Evaluation

The basic concepts of reliability evaluation based on stress-strength interference (**SSI**) theory are that a given component has a certain strength which, if exceeded by the stress, will result in the failure of the component.

https://doi.org/10.1017/jmech.2016.96 Published online by Cambridge University Press

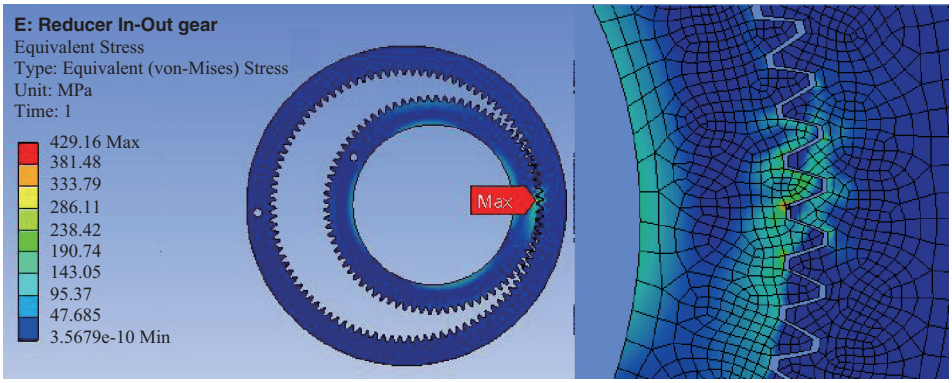


Fig. 9 Equivalent stresses.

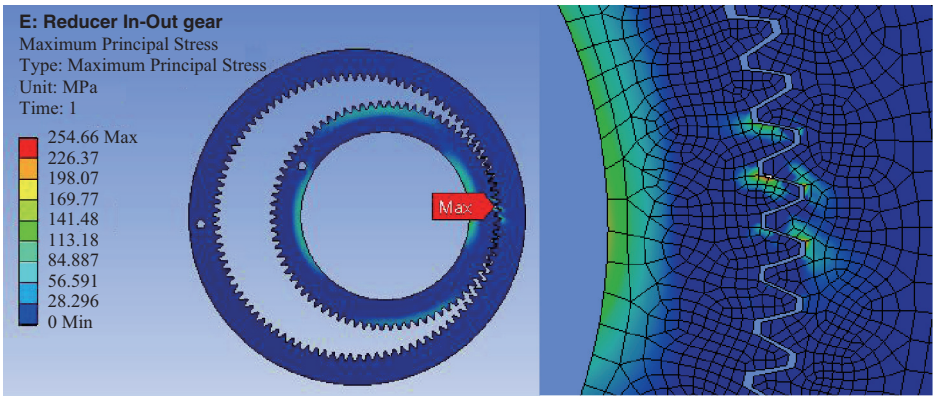


Fig. 10 Maximum principle stresses.

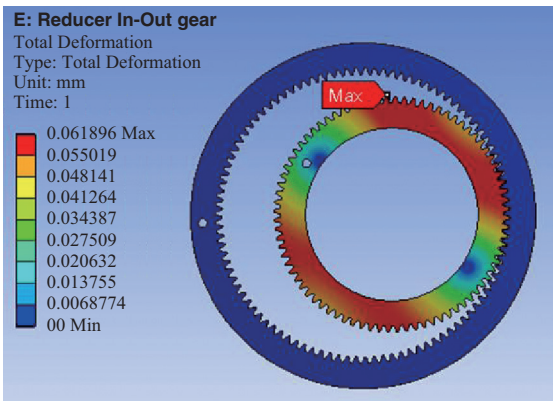


Fig. 11 Total deformations.

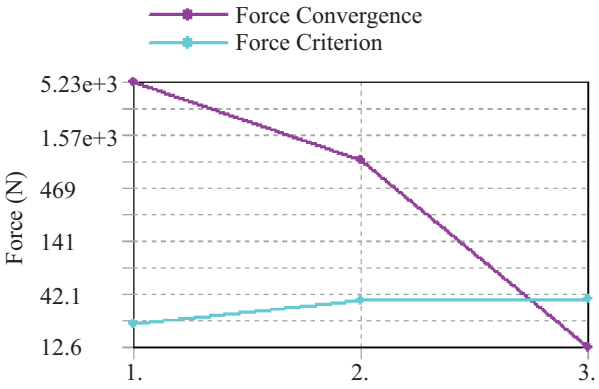


Fig. 12 Force convergence.

The strength and the stress (or acting loads) of the component are expressed as random variables. Stress is used to indicate any agency that tends to induce failure, while strength indicates any agency that resists failure. Failure means that the functions do not meet the intended specifications and is defined to have occurred when the actual stress exceeds the actual strength for the first time.

The reliability index can be calculated based on the second-order moment method if the strength random variable X is normally distributed with a mean value of μ_X and standard deviation of σ_X, and the stress random variable Y is also normally distributed with parameters μ_Y and σ_Y. The reliability index, z, can be measured by

$$z = \frac{\mu_X - \mu_Y}{\sqrt{\sigma_X^2 + \sigma_Y^2}}. \tag{7}$$

The reliability can be expressed as

$$R = 1 - \Phi(-z) = \Phi(z). \tag{8}$$

where $\Phi(\,)$ means the cumulative distribution function of normal distribution. A typical target value for reliability index $\mathbf{z = 3}$ is the reliability $\mathbf{R = 0.99865}$.

For structural system, the induced stress (μ_Y, σ_Y) would be the designed variants if the strength information of materials (μ_X, σ_X) is known. While the variation

https://doi.org/10.1017/jmech.2016.96 Published online by Cambridge University Press

Table 3 The analyzed results at various element sizes

Element size (mm)	Mesh Nodes	Mesh Elements	Equivalent stress (Mpa)	Principal Stress
2	4482	1200	232.84	153.08
1.5	4959	1325	280.81	184.93
1	5736	1580	329.90	211.59
0.8	6362	1762	371.00	225.15
0.5	8474	2464	401.50	244.50
0.3	9233	2707	417.04	249.88
0.2	9604	2828	424.49	252.79
0.1	**10141**	**2991**	**429.16**	**254.66**

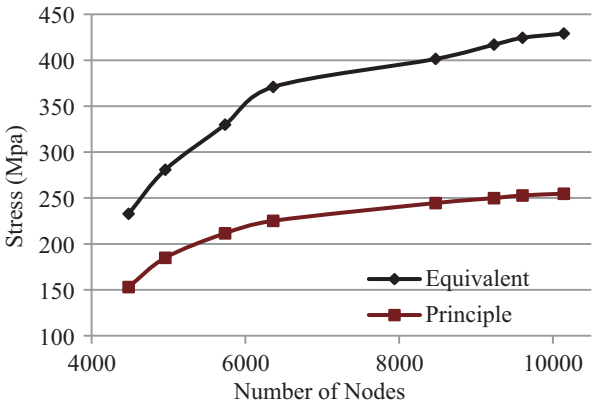


Fig. 13 Convergence study.

coefficients of the designed variants γ_Y are known, the standard deviation of the induced stress can be evaluated by

$$\sigma_Y = \gamma_Y \mu_Y \tag{9}$$

Substituting Eq. (9) into Eq. (7), we can derive the following equation when the reliability target is set to R $\geqq$ Φ(z).

$$[1-(\gamma_Y z)^2]\mu_Y^2 - 2\mu_X\mu_Y + \mu_X^2 - (\sigma_X z)^2 \geq 0 \tag{10}$$

Solving the above equation, the design solution for the induced stress must satisfy the condition

$$\mu_Y \leq \frac{\mu_X - \sqrt{\mu_X^2 - (1-\gamma_Y^2 z^2)(\mu_X^2 - \sigma_X^2 z^2)}}{1-\gamma_Y^2 z^2} \tag{11}$$

The variant coefficients γ_Y can be decided by the means and the variations of the variables in the stress equation. For example, (F, A) representing the force and the area of a design, the mean of the stress would be $\mu_Y = \mu_F/\mu_A$. The variation coefficient would be $\gamma_Y^2 = \gamma_F^2+\gamma_A^2$. No sooner than the γ_Y decided, the allowed value of the induced stress can be computed by Eq. (11) when the strength information and the needed reliability are given. This form is commonly adopted when the performance index belongs to the-smaller-the-better.

On the other hand, if the known information is the expected performances given direct by the customers (the requirement marked as Y), the designed variant would be the real performance of the design (the supply marked as X). Likely, the following equation is derived as

$$[1-(\gamma_X z)^2]\mu_X^2 - 2\mu_Y\mu_X + \mu_Y^2 - (\sigma_Y z)^2 \geq 0 \tag{12}$$

The design solution for the strength must satisfy

$$\mu_X \geq \frac{\mu_Y + \sqrt{\mu_Y^2 - (1-\gamma_X^2 z^2)(\mu_Y^2 - \sigma_Y^2 z^2)}}{1-\gamma_X^2 z^2} \tag{13}$$

Here, γ_X represents the same behavior as γ_Y. The performance of design supply μ_X must satisfy above equation. This form is usually used when the performance index is the-bigger-the-better.

5. 2 Reliability of DR

Reliability evaluation of **DR** deals with probabilistic distributions of the strengths and the stresses. The strengths can be acquired by querying the mechanical properties of materials. In this paper, the materials of the gear rings are designed with structural steel, S35C where the tensile and yielding strengths are 510 MPa and 304 MPa, respectively. The allowable stresses of gears can query the technical notes of Japanese Gear Manufacturer Association (JGMA), JGMA 402-01 [10]. The specifications introduced the methods of calculating bending and surface-durability stresses of spur gears and helical gears. The allowable stresses are also suggested in the specifications. According to the data, the allowable bending and contact stresses of material S35C are about at **180 MPa** and **490 MPa**, respectively. Comparing the material strengths and the allowable stresses, we can draw out a relationship that the allowable bending stress is about at one third of the tensile strength, and the allowable contact stress is about equal to the tensile strength.

Reviewing the analyzed maximum stresses in bending and contacting, we can conclude that the bending fracture of the gear rings would occur prior to the contact fractures since the bending stresses has been over the allowable value. As a result, the reliabilities of the **DR** would be evaluated based on its bending stresses. The bending strengths of the gear rings are set to the yielding stress of materials. The means and standard deviations of bending strengths are set to (μ_X, σ_X) = (304, 30.4) MPa for considering 10 percents of strength variation. Combining the strengths and the analyzed stresses obtained by **FTA**, the reliabilities of the **DR** can be evaluated by Eq. (8). Typically, the reliabilities of the **DR** at the input loadings **200 Nm** (the bending stresses 252 MPa) would be **R = 0.956**. On the other hand, the allowed maximum bending stresses of the gear rings can be decided subjected to the set reliability needs by Eq. (11). For example, the allowed stress is **233** MPa if the reliability need is **R = 0.99** for the stress variation is set to 0. Further, the allowed input torques of the **DR** can also be evaluated by the stress information.

https://doi.org/10.1017/jmech.2016.96 Published online by Cambridge University Press

Here, the allowable loadings of the **DR** are decided according to the evaluations of the maximum bending and contact stresses of the gear rings obtained by **FEA**. The acted loadings and the maximum stresses at various input torques are listed in Table. 4. Considering the allowable stresses defined in JGMA, the allowed input torques of the **DR** would be about at **130 Nm** and the fracture torque would be about at **240 Nm**, i.e. the maximum bending stress reachs to the yielding point.

Table 4 Bending and contact stresses under different input torques

Input torques T1(Nm)	T2(Nm)	F(N)	Bending (MPa)	Contacting (MPa)
100	80	2000	151	252
120	96	2400	173	289
140	112	2800	193	324
160	128	3200	212	358
180	144	3600	232	391
200	160	4000	255	429
220	176	4400	285	462
240	**192**	**4800**	**316**	**495**
260	208	5200	348	528
280	224	5600	375	558
300	240	6000	398	586

The reliabilities of the design at various input torques are further evaluated based on the **SSI** theory according to the analyzed results on bending stress. The reliability changing with respect to the loading torques is shown in Fig. 14. The results show a steeper changing of reliability degradation when the stress variation is considered with ry = 0. The reliabilities would be changed while the variations on the strength and the stress are set to different values. The analyzed results offer the reliability information of the **DR** depending upon the loading torques so that the allowed input torques at various reliabilities can be determined accordingly.

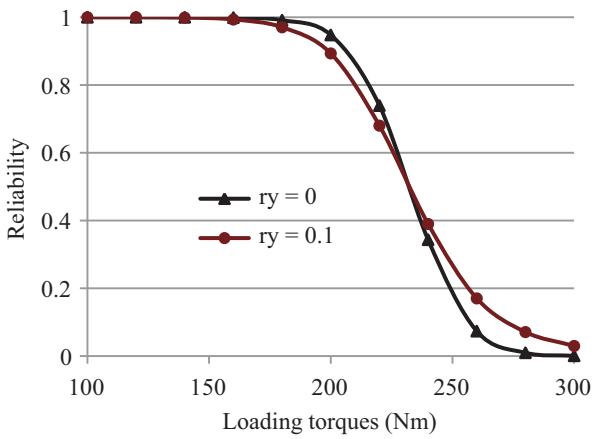


Fig. 14 Reliabilities of the reducer at various loadings.

6. CONCLUSIONS

This paper presents a new design of speed reducers which own the properties, high rigidness, large speed reduction ratios and compact structure. The mechanism is designed based on differential displacements of the decelerated gear rings. The geometric models of structure are designed by SolidWorks software for performing interference checking, motion analysis and structural stress analysis. The mathematical models of gear stress are proposed based on ISO 6336 standards for evaluating the bending and contact stresses. The maximum bending and contact stresses of the gear rings are further analyzed using **ANSYS**. The analyzed results show that the bending stress fractures would prior to its contact stress failures so that the allowable loadings of the **DR** can be determined according to its bending strengths. The convergence analysis of stresses in **FEA** shows that the analyzed results are acceptable. The methods of reliability evaluation are proposed to picture out the reliabilities of the **DR** under various loading torques. The studied results provide the useful information for structural design, stress analysis and reliability evaluation on developing a reducer owning high speed-reduction ratios.

ACKNOWLEDGEMENTS

The work was supported by a grant from the Ministry of Science and Technology under contract No: MOST 103-2221-E-237-002.

REFERENCES

1. Ono, K., Hayashi, T., Fujii, T. M. and Shibasaki N., "Development for Industrial Robotics Applications," *IHI Engineering Review*, **42**, pp. 103-107 (2009).
2. Taghirad, H. D. and Belanger, P. R., "Modeling and Parameter Identification of Harmonic Drive Systems," *Journal of Dynamic Systems, Measurement and Control*, **120**, pp. 439-444 (2009).
3. Ghorbel, F. H., Gandi, P. S. and Alpeter, F., "On the Kinematics Error in Harmonic Drive Gears," *Journal of Mechanical Design*, **123**, pp. 90-97 (2001).
4. Li, S. T., "Design and Strength Analysis Methods of The Trochoidal Gear Reducers," *Mechanism and Machine Theory*, **81**, pp. 140-154 (2014).
5. Marciniec, A. and Pawlowicz, A., "The Bending and Contact Stress Analysis of Spur Gears," *Journal of KONES Powertrain and Transport*, **16**, pp. 243-250 (2009).
6. Koisha, J. R. and Doshi, H. P., "Influence of Friction on Contact Stress for Small Power Transmission Planetary Gear Box", *International Journal of Engineering Research and Development*, **1**, pp. 38-43 (2012).

https://doi.org/10.1017/jmech.2016.96 Published online by Cambridge University Press

7. *Calculation of Load Capacity of Spur and Helical Gears - Part 1: basic principle, introduction and general influence factors*, International Standard ISO 6336/1, pp. 1-100 (1993).
8. *Calculation of Load Capacity of Spur and Helical Gears - Part 2: calculation of surface durability (pitting)*, International Standard ISO 6336/2, pp. 1-28 (2006).
9. *Calculation of Load Capacity of Spur and Helical Gears - Part 3: Calculation of tooth strength*, International Standard ISO 6336/3, pp. 1-72 (1993).
10. *Surface Durability Formula of Spur Gears and Helical Gears,* JGMA 402-01, Japanese Gear Manufacturer Association (JGMA), (1975).
11. Cook, R. D., *Concepts and Applications of Finite Element Analysis*, John Wiley & Sons, Inc., New York (2001).
12. *ANSYS user's manual*, ANSYS Inc., Canonsburg (2012).
13. Tsai, Y. T. and Chang, H. C., "Reliability-Based Optimum Design for Mechanical Problems Using Genetic Algorithms," *Proceedings of the Institution of Mechanical Engineers, Part C: Journal of Mechanical Engineering Science*, **222**, pp. 1791-1799 (2008).
14. Tsai, Y. T., Wang, K. S. and Woo, J. C., "Fatigue-Life and Reliability Evaluations of Dental Implants Based on Computer Simulation and Limited Test Data," *Proceedings of the Institution of Mechanical Engineers, Part C: Journal of Mechanical Engineering Science*, **227**, pp. 554-564 (2013).
15. Tsai, Y. T., Lin, K. H. and Hsu, Y. Y., "Reliability design optimisation for practical applications based on modelling processes", *Journal of Engineering Design*, **24**, pp. 849-863 (2013).
16. Yang, Y. H., Tsai Y. Y. and Wang, W. S., "The Characteristic of cumulative damage study about electric insulation based on Accelerated life tests", *Journal of Mechanics*, **30**, pp. 11-19 (2014).
17. Tsai, Y. T. and Wang, K. S., "A study of reliability analysis of fatigue life for dental implants", *Journal of Chinese Society of Mechanical Engineers*, **36**, pp. 439-448 (2015).

(Manuscript received April 29, 2016,
accepted for publication Julyl 19, 2016.)

https://doi.org/10.1017/jmech.2016.96 Published online by Cambridge University Press